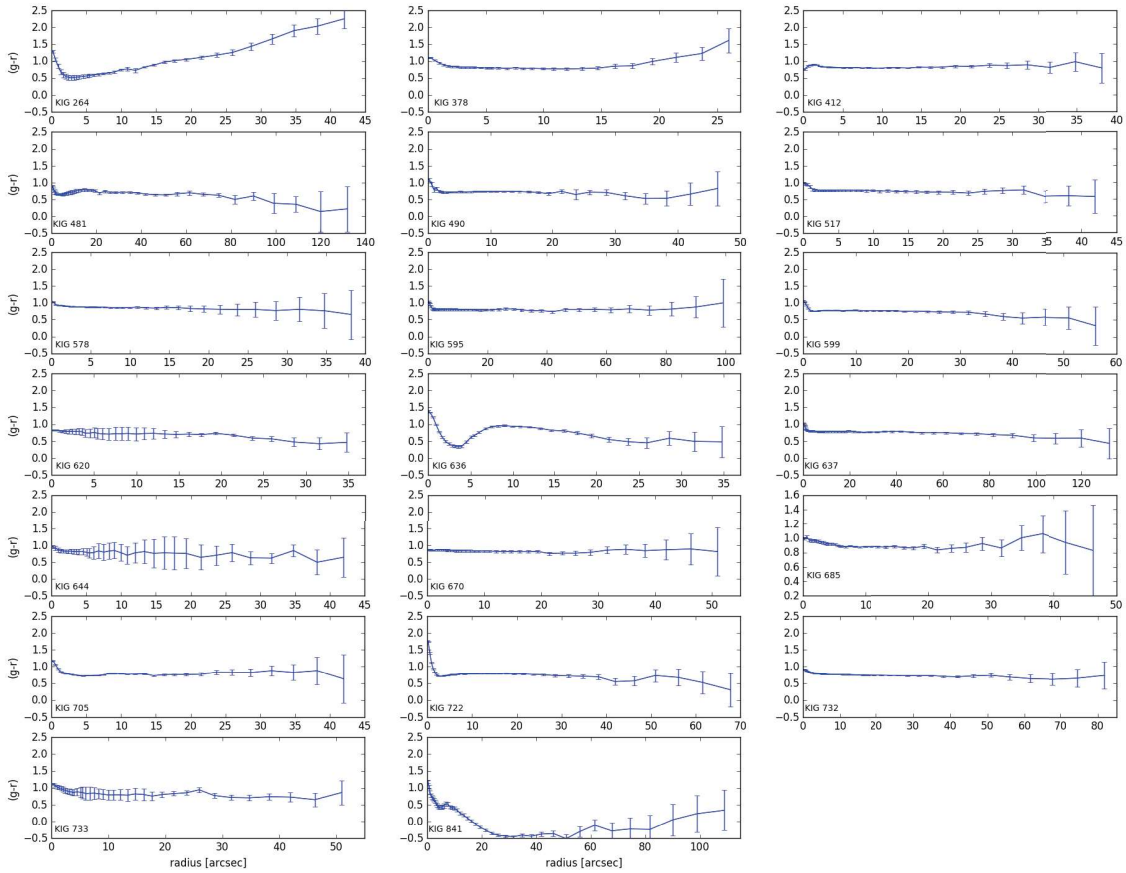

Fig. 7. Galaxy $(g - r)$ colour profiles. Single profiles are presented and discussed in Sect. 4.2.

although the model tends to overestimate the galaxy luminosity in the outskirts. The bulge dominates in the adopted B+D best fit. It remains unclear why the B/T light ratio, which is 0.63 in g and 0.78 in r, differ so much although the fit is good in both cases. A residual structure (a tail?) extending from the nucleus towards the NW, which is particularly evident in the r band, is revealed after the model subtraction. We classify this galaxy as S0 pec, taking into account the asymmetric residual structure. The $(g - r)$ profile is nearly flat at about 0.8 mag up to 17″, and then it becomes redder and reaches ≈1 mag at about 20″ , where there are significant measurement errors, however.

KIG 412. The galaxy is one of the less isolated galaxies in the sample (Fig. 2) for Verley et al. (2007a), but the spectroscopic criterion of Argudo-Fernàndez et al. (2013) is fulfilled. All classifications in Table 1 converge in indicating this galaxy is an E, but it is an S0 galaxy for H-T. The single Sérsic fit provides $n = 4.38 \pm 0.11$ and $n = 5.80 \pm 0.02$ in g and r bands, respectively. However, this model not only overestimates the luminosity in the galaxy light profile in the outskirts, but the trend of the residuals also suggests the presence of a second component. The B+D provides a statistically better fit (Fig. A.1 bottom panel), as in the case of KIG 378. The residuals after the B+D model subtraction show a faint inner ring and a ring or shell-like structure in the outskirts (similar to KIG 685). Although this latter structure is revealed below 2σ of the sky level, it is evident in both original images, especially in the r band, starting from ≈20″. Our surface photometry supports an E/S0 pec classification because the bulge is still dominant; B/T is 0.69 and 0.71 in the g and r bands, respectively, and residual structures are present. The $(g - r)$ colour profile is nearly flat at about 0.8 mag.

KIG 481. The galaxy has a very uncertain classification. It is an SA ($T = 1$) for Buta et al. (2019), an Sab for H-T, a late S0 ($T = -0.1$) for `HyperLeda`, and a classic S0 ($T = -2$) for Fernandez-Lorenzo et al. (2012). Morales et al. (2018) found two classical shells on either side of the galaxy. Our best fit (Fig. A.2) is obtained using a B+D model with a $B/T = 0.66$ and $B/T = 0.69$ in g and r bands, respectively. Residuals show a strong irregular dust-lane and a wide system of three nearly concentric shells. We suggest that it is a S0 pec (see also Buta et al. 2019). The galaxy $(g - r)$ colour profile is quite blue in the galaxy centre, it is 0.64–0.7 mag, and it tends to become bluer with radius.

KIG 490. The galaxy is considered a late-S0 (Table 1) and an Sa for H-T. In Fig. A.2 we show our B+D best fit of the galaxy light profile. Residuals show a wide plume, likely a tail, in the NE part of the galaxy starting at about 30″ from the nucleus. The feature is reminiscent of the fan or tail found on the NW side of KIG 264 and connected with the shell. The B/T ratio (0.50 in g and 0.53 in r) together with the ripple and tail we detected fully justify the Buta et al. (2019) classification of a late, un-barred, and peculiar S0. The $(g - r)$≈0.74 mag colour profile is typical of ETGs (Fig. 8 bottom panel).

KIG 517. This galaxy is considered a classical E by Buta et al. (2019) and H-T and an S0 by `HyperLeda` and Fernandez-Lorenzo et al. (2012). H-T found that it has a boxy structure that

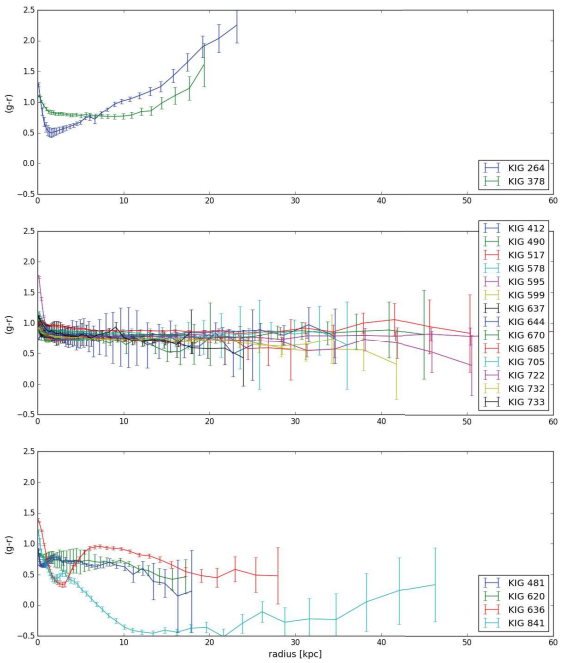

Fig. 8. $(g-r)$ colour profiles in kpc (using the galaxy distance provided in Table 1). Colour profiles have been subdivided into three classes according to their behaviour outside the seeing-dominated area: galaxies with colour profiles become redder with radius (*top panel*), flat colour profiles (*middle panel*), and colour profiles with a peculiar behaviour or that become bluer in the outskirts (*bottom panel*).

we do not see in either the original isophotes or as an artefact in the residuals. The single Sérsic best fit provides n values near to a de Vaucouleurs law. Our B+D model (Table 4) subtraction (Fig. A.3) shows a faint residual ring in the range 5–10″. The B/T values are 0.71 and 0.74 in g and r, respectively, indicating a large bulge contribution. We suggest that the galaxy is an E/S0. The $(g-r)$ colour profile is flat around 0.75 mag.

KIG 578. The galaxy is classified E by all authors in Table 1 and by H-T, who detect a discy structure in isophotal shape profiles. The best fit is obtained with a single Sérsic law, with $n \approx 4$; the B+D model best fit is statistically poorer. The residuals after model subtraction shown in Fig. A.3 reveal a ring between ≈10″-20″ and a faint outer ring or shell-like structure, detected at 2σ of the sky level, in the galaxy outskirts. KIG 578 is in the bona fide Es sample of H-T, and they did not detect shells in their SDSS image. We suggest that KIG 578 is a peculiar elliptical. The $(g-r)$ colour profile is flat around 0.86 mag.

KIG 595. The galaxy is classified an E by Buta et al. (2019) and `HyperLeda` and as an S0 by Fernandez-Lorenzo et al. (2012) and as an SAB0 by H-T. The light profile is best fitted by a B+D model with a $B/T = 0.78$ in both bands. The residuals in Fig. A.4 show a faint inner ring and a series of shells that connects in the north to a tail (below 2σ level) that extends to the NW. No bar is revealed. We suggest that the galaxy is an E/S0 peculiar. The $(g-r)$ colour profile is flat around 0.80 mag.

KIG 599. Classifications in Table 2 see the galaxy as a S0, but it is an E with discy isophotes and a system of shells and ring for H-T. A B+D model fits the galaxy best. Residuals after model subtraction show an arm-like structure in the inner part, and shells and a faint ripple on the SE side of the galaxy, emerging at about 40″ in both bands (Fig. A.4). We suggest that the galaxy is a peculiar S0, likely late, because $B/T = 0.39$ as in Fernandez-Lorenzo et al. (2012). The $(g-r)$ colour profile is flat around 0.77 mag.

KIG 620. The morphological type of this galaxy ranges from −2 to 1 ± 1.6, suggesting that its is a late-S0 or an early spiral. According to `HyperLeda`, the galaxy hosts a bar. H-T classifies the galaxy as an early spiral ($T = 0.69$). Our image shows that KIG 620 is composed of a inner disc, seen nearly edge-on, with $\epsilon = 0.72$, which is embedded in a diffuse nearly round structure (top panels in Fig. A.5). The Sérsic and B+D models both provide a poor fit: the bulge is small, and the parameters are largely contaminated by the inner ring. We support the Buta et al. (2019) classification because we do not see a bar. No fine structures are detected at a significant level. KIG 620 is reminiscent of 3D early-type galaxies reported in Buta et al. (2015), whose prototypes are shown in their Fig. 23. The $(g-r)$ colour profile is flat around 0.72 mag and tends to become bluer aound 0.5 in the outskirts, although the errors are large.

KIG 636. The galaxy is considered an S0 by the tree classifications in Table 2. It has a bar both for Buta et al. (2019) and for the `HyperLeda` classification. H-T classified the galaxy as E. Residuals from a Sérsic or a B+D model show the effect of a small bar or lens (clearly visible in the original central isophotes in both bands), and an outer ring from which extended arm-like structures (tails?) depart, with arms on the E and W sides of the galaxy. The bulge parameters are contaminated by the bar in this case as well. We modelled the galaxy to enhance the outer galaxy structures. The classification of Buta et al. (2019) describes the inner morphology of the galaxy ($T = -2.5$) well, $B/T = 0.74$ would suggest $T = -3$ of Fernandez-Lorenzo et al. (2012). The suffix "pec" is necessary because of the arm-like residual structures. The increasing reddening, from ≈0.4 to 1 mag, of the $(g-r)$ colour profile is connected to structures detected in the residuals map up to about 10″. After this, the $(g-r)$ trend inverts and becomes increasingly blue. It reaches 0.6–0.5 mag, although with large errors, in correspondence to the outer ring and arm-like structures.

KIG 637. The galaxy is classified as an elliptical in Table 1. Recently, Costantin et al. (2018) reported the i- SDSS band surface photometry of this galaxy (NGC 5687 in the paper) and found that it is an S0 whose bulge can be unambiguously classified as classical ($n > 2$), with an $n = 2.58 \pm 0.0$. This galaxy was chosen by Costantin et al. (2018) because it is unbarred.

Several bright stars in the field, in particular, HD238370, which generates a very extended corona, hampered the surface photometry and the estimate of the value of the total integrated magnitudes provided in Table 4. The galaxy extends ≈2.5′ in radius. We fit the entire light profile with a Sérsic law ($n = 3.92$ and $n = 4.09$ in the g and r bands, respectively). The index would suggest a classical E galaxy. However, the B+D model provides a better fit of the light profile. Residuals reveal a ring structure in the galaxy centre. This does not seem an artefact because this feature is also visible in i bands by Costantin et al. (2018) after the subtraction of their Sérsic+exponential disc model. Our measured PA=102° and ellipticity $\epsilon = 0.39$ (see Table 4) agrees with those found by the above authors. We suggest that the galaxy is an S0 ($B/T = 0.57$) whose inner and outer rings are revealed by the residuals. The $(g-r)$ colour profile is nearly flat at ≈0.78–0.74 mag, without a signature of the structure detected in the residuals, and it tends to become bluer in the outskirts and reaches 0.6 mag with large errors.

KIG 644. The galaxy morphological type has a wide range of variation $-1 \leq T \leq 2.2$. The galaxy is considered borderline with a spiral: H-T classified it as Sab(s). As in the case of KIG 620, we failed to fit the light profile: both Sérsic and B+D model offer quite a poor fit. In the inner regions lies a ring-like structure with a diameter of about 10″ that hampered the fit of a very small bulge. Our images reveal neither spiral arms, as assumed by HyperLeda and H-T, nor fine structures such as shells and tails in the outskirts. We consider the classification provided by Buta et al. (2019) adequeate. The authors suggested a ring-like feature that outlines a bar that might be related to the x_1 family of bar orbits as in NGC 6012 (see e.g. Buta et al. 2015, for an explanation). We assigned S0 as the morphological class. The $(g-r)$ colour profile is nearly flat around 0.77 mag with large errors, without a signature of a ring.

KIG 670. The galaxy classification ranges from pure E to classic S0. A B+D model fits the light profile best. After model subtraction, the residuals show central asymmetries that are due to isophote twisting that is not accounted for in the model. In the outskirts, however, asymmetries (shells or ripples?) are visible in both bands (Fig. A.6). We suggest that the galaxy is an E/S0 pec as a consequence of a $B/T = 0.73$ and of the peculiar outskirts. The $(g-r)$ colour profile is nearly flat around 0.82 mag.

KIG 685. The galaxy is considered a bona fide elliptical. H-T considered the galaxy an S0, however. Rampazzo et al. (2019) fit the high-resolution (PSF = 0.″25) K-band 2D light distribution best with GALFIT, adopting a model composed of two Sérsic laws representing a pseudo-bulge ($n = 2.95 \pm 0.10$) plus a disc ($n = 0.78 \pm 0.10$). The ellipticity profile, showing two regimes, suggested the presence of the disc. KIG 685 K-band residuals show ring and shell-like structures. Our surface photometry is heavily hampered by bright stars that are located very near the galaxy centre. The PSF (see Table 3) is between 3.5 (g band) and 4.8 (r band) times that of ARGOS+LUCI adaptive optics instrument at the LBT. Our g and r study confirms the disc, the shell and ring-like structures that were detected in the previous study, as shown in Fig. A.6. We suggest that the galaxy is a peculiar E/S0. The $(g-r)$ colour profiles is nearly flat at ≈0.88 mag.

KIG 705. This galaxy is also considered an E (see Table 2), including H-T, who in addition reported a discy structure of the isophotes, an inner disc, and shells and ripples. A Sérsic model fits the galaxy best, with $n = 3.61 \pm 0.03$ in g and $n = 4.07 \pm 0.08$ in r, supporting the idea that this is a classic E (top panels of Figures A.8). The B+D model, which is statistically indistinguishable from the previous model, offers a $B/T = 0.89$ in both bands, suggesting in any case that the bulge component is dominant. The residuals after model subtraction enhance shells and ripples in the galaxy outskirts. The galaxy shows a disc-like structure in the inner region. We assigned E pec as the morphological class. The $(g-r)$ colour profiles are nearly flat around 0.77 mag.

KIG 722. The galaxy is considered a bona fide E with boxy isophotes according to H-T. Our best-fit model is a Sérsic law in both bands with exponents near the classic de Vaucouleurs law (see Table 4). The residuals (bottom panels of Fig. A.8) in the central part of the galaxy therefore are an artefact created by the combination of the isophote twisting and boxiness with respect to the model. The excesses of light between 20″-40″ at the NE and SW sides of the galaxy appear as real fans and shells that are also visible in the original image. H-T did not detect shells in their SDSS image of KIG 722. We assigned E pec as the morphological class. The $(g-r)$ colour profiles are nearly flat around 0.76 mag without any obvious connection with the structure that is enhanced by the residuals.

KIG 732. This galaxy is another bona fide E in Table 2. H-T reported that this E has a boxy structure, dust, and possibly an inner disc. Our best-fit model is the B+D shown in Fig. A.9, although the bulge predominates ($B/T = 0.88$ and 0.78 in g and r bands). Isophotes appear strongly boxy: this is the reason for the cross-like residuals in the central regions of the galaxy. The residuals also enhance shells and a spiral-like structure that is likely due to isophote twist and extends out to the galaxy outskirts. We assigned the E/S0 pec morphological class. There are no traces in the nearly flat (around 0.77 mag) $(g-r)$ colour profile of the structures that are traced by the residuals. H-T did not detect shells in their SDSS image of KIG 732.

KIG 733. The galaxy is borderline, with an early spiral ($0 \leq T \leq 1.5$) in the classifications provided in Table 1. Our B+D model fails to provide an adequate fit to the light profiles (bottom right panel in Fig. A.9). The galaxy has a complex morphology that is well described by the classification of Buta et al. (2019), with an outer ring starting from wide open arms. There is dust along the arms that appears knotty (see the bottom left panel). Considered as a whole, the galaxy is reminiscent of the 3D early-type objects in Buta et al. (2015), similarly to KIG 620. We suggest that the correct classification is provided Buta et al. (2019), so we assigned S0 pec as the morphological class. The $(g-r)$ is red, nearly flat around 0.8 mag, with a mini peak of 0.94 mag at about 26″ in correspondence of the outer ring.

KIG 841. The galaxy is considered late-S0 ($T = 0$) in Fernandez-Lorenzo et al. (2012). For Buta et al. (2019), is also an S0, but with several peculiar features, such as an inner ring and plume, while it is an E/S0 for HyperLeda. Our surface photometry confirms the peculiar features in the Buta et al. (2019) classification. Furthermore, we find evidence of a wide systems of shells that is particularly evident on the NE side. Our best fit is obtained with a B+D model. The outer shells appear as an increase in luminosity in the model at ≈70″ at about 27 mag arcsec^{-2} in g band and 26 mag arcsec^{-2} in r band. We classify this galaxy as a late-S0 pec because $B/T \approx 0.6$. The $(g-r)$ colour profile (Fig. 8) is entirely unexpected for ETGs. Outside the seeing, it has values of about 0.6 mag, then it becomes increasingly bluer up to 25″ , with a flat part at about −0.4 mag up to 50″. In the galaxy outskirts, the $(g-r)$ trend turns to red, but the values are still below 0 mag.

To summarise, our light profiles reached on average $\mu_g = 28.11 \pm 0.7$ mag arcsec^{-2} and $\mu_r = 27.36 \pm 0.68$ mag arcsec^{-2}. The results of the light-profile analysis decomposition are listed in Table 4. A minority, 15% (3 out of 20), of our iETGs can be considered bona fide Es that are fitted best by a Sérsic law with the exponent $n \approx 4$, that is, by a de Vaucouleurs law. For the vast majority, the B+D model fits the galaxy light profile best. The bulge flux is dominant, with an average $B/T \approx 0.66$ in both bands. Three out of 20 iETGs, that is, NGC 620, NGC 644, and NGC 733, are late S0s at the border with spirals, some showing arm-like structures in their central region, as in the Buta et al. (2019) classification. On the whole, their morphology is reminiscent of the 3D ETG class described in Buta et al. (2015). We conclude that our sample is composed of bona fide ETGs.

After the 2D model was subtracted, most of the galaxies showed fine structures that emerged in their inner regions and outskirts. In particular, 12 out of 20 iETGs (60%) showed clear evidence of shell and ripple signatures (Table 4, Fig. 5, and Figs. A.1–A.9). None of the late S0s mentioned above show

shells, ripples, or tails. In Sect. 2.2 we discussed the revised isolation criteria for the galaxy in the sample performed by Verley et al. (2007a) and Argudo-Fernàndez et al. (2013). Figure 2 shows that all iETGs with shells except for KIG 412 and KIG 595 lie within the fiducial range of isolation in the η_k-Q plane. This means that the fraction of shell galaxies within the isolation fiducial range reaches 62% (10 out of 16).

Most of the colour profiles, 13 out of 20 (65%), are flat with values in $(g-r)$ of about 0.7–0.8 mag, which is typical of ETGs. Ten of the 12 shell galaxies have red $(g-r)$ colour profiles; 2 galaxies, KIG 481 and KIG 841, have blue (and peculiar, in particular, KIG 841) colour profiles.

5. Discussion

By definition, iETGs are early-type galaxies without obvious companions. Considering the above results, the question is how long isolated early-type galaxies have been isolated. The answer, which involves both the timing and the physical mechanisms driving the iETG evolution, can be approached using the various fine structures that are detected as markers, together with other indicators that we discuss in the following sections.

5.1. Shapes of the residuals

Simulations suggest that the fine structures revealed by our surface photometry are connected to past interacting and merging history. We review the residual shapes and discuss them in the light of the literature.

5.1.1. Shells

In the literature, shells have been widely associated with both minor and major and both wet and dry merging episodes (see e.g. Dupraz & Combes 1987; Weil & Hernquist 1993; Mancillas et al. 2019; Pop et al. 2018, and references therein). Several studies have suggested that the fraction of shells, and in general, the fraction of tidal features, indicate a strong environmental effect. Reduzzi et al. (1996) found that about 16.5% of ETGs in the field showed shells, which is at odds with the hypothesis that 4% of ETGs are members of physical pairs. Only 4% of the shell galaxies in the original Malin & Carter (1983) list are located in clusters or rich groups. An incidence of 50% of shells has been found by H-T in 18 isolated galaxies that they considered bona fide Es, using the SDSS DR6 data set.

Our set of galaxies, however, needs to be compared with results from deep surface photometry because the fraction of detected features certainly depends on this factor. Tal et al. (2009) investigated a complete volume -limited (15–50 Mpc) sample of bright ($M_B < -20$) ETGs and detected 12 out of 55 (22%) objects with shells. Their surface brightness reached 27.7 mag arcsec^{-2} in the V band. The authors noted that the fraction of galaxies with tidal features increased and did not include cluster members. We found that about 60% of our iETGs shows shell structures. With respect to H-T, we revealed shells also in KIG 264, KIG 578, KIG 722, and KIG 732, which are all included in their sample of isolated Es. Recently, Pop et al. (2018) investigated shells in 220 of the most massive galaxies, regardless of their environment, in the `Illustris` simulation (Genel 2014; Vogelsberger 2014a,b). They reported shells in 39 galaxies, which is 18 ± 3%. This fraction is consistent with the fraction found by Tal et al. (2009). The fraction of our iETGs that shows shells is three times greater than that found by Tal et al. (2009).

Most (9 out of 13) iETGs with shells have flat and red $(g-r)$ colour profiles. This is consistent with the general finding that shells are more common in red than blue (spiral) galaxies (see e.g. Atkinson et al. 2013). KIG 481 and KIG 841, which have blue colour profiles, are still in the green valley (see Sect. 5.3).

The Mancillas et al. (2019) simulations suggested that shells are a long-lasting feature (see also Longhetti et al. 1999; Rampazzo et al. 2007). The estimated survival time of shells is ≈3 Gyr. Lacking possible perturbers, shells in our iETGs were generated by the last merging event and set the isolation time, which is of that order. Shells basically disappear in cluster ETGs, which likely is a consequence of the galaxy transformation due to continuous harassment processes (Moore et al. 1998). In less isolated ETGs (see Sect. 2.2), the fraction of galaxies with shells is still higher than the fraction quoted by Tal et al. (2009). Further indications about the age of the interaction are developed in Sect. 5.3.

Two of the iETGs with shells deserve further attention. KIG 264 shows a system of shells and a ripple that is reminiscent of a tail (Fig. 5). The galaxy has been studied at radio wavelength by Wong et al. (2015). They described KIG 264 (identified as J0836+30 in their paper) as the more passive object in their sample. They did not detect nuclear radio emission in the galaxy at 1.4 Ghz, but observed two radio lobes at 88.4 kpc north-west and 102.5 kpc south-east of the galaxy centre. In the direction connecting the two radio lobes, they detected an extragalactic H I cloud midway between the galaxy centre and the lobe on the north-west side (see their Figs. 2 and 5). Wong et al. (2015) suggested that an active central engine has the required energy to expel gas from the galaxy because two radio lobes are located in the same direction as the H I cloud. KIG 264 likely hosted a radio AGN that may have blown out the observed gas cloud.

Our surface photometry shows that KIG 264 has no bar that would drive gas to the centre. The wide system of shells extends to almost include the H I cloud. Because shells and ripples are the scars of a recent merging (see e.g. Mancillas et al. 2019), we suggest that this event has likely involved gas-rich galaxies (wet merging) and might have activated the past AGN activity in KIG 264.

KIG 264 shows the remains of the AGN activity, and the processes may occur during a merging episode. Bennert et al. (2008) found several cases of (active) AGN host galaxies with an underlying shell system. On the other hand, Hernàndez-Ibarra et al. (2013) found low AGN-level activity in our iETGs sample: only three galaxies, KIG 378, KIG 595, and KIG 705, have a low ionization nuclear emission line region (LINER) in the nucleus.

The other interesting case is KIG 841 (NGC 6524). The type Ia pec supernova SN2010hh exploded in its shell (Marion 2010; Silverman et al. 2010) (SN1991bg-like). The progenitors of this type of supernova are old stars, that is, stars that were likely re-distributed from the parent galaxies during the merging episode.

5.1.2. Tails, plumes, and fans

Tails of stellar matter are generated by interaction and merging phenomena (see e.g. Mancillas et al. 2019, and references therein). Broad stellar fans are also generated by interaction (see e.g. Tal et al. 2009). The tail survival time is ≈2 Gyr, while streams remain visible in all phases of galaxy evolution. Streams, however, are detected in simulations at very low levels of surface brightness. The Mancillas et al. (2019) simulations revealed between two and three times more streams with a surface brightness cut of 33 mag arcsec^{-2} than with 29 mag arcsec^{-2}.

Tal et al. (2009) found that tails are less frequent than shells in ETGs: they found tails in 13% (7 out of 55) of the ETGs. Tails exist for shorter times than shells (Mancillas et al. 2019). Tails tend to indicate a recent encounter and/or merging. Furthermore, tails are evidence for a dynamically cold component (e.g. a disc).

We consider as tails, fans and plumes the features found in KIG 264, KIG 378, KIG 490, KIG 595, and KIG 636, that is, 25% (5 out of 20) of our sample. KIG 378, KIG 490, and KIG 636 were considered isolated by both Verley et al. (2007a) and Argudo-Fernàndez et al. (2013). All these galaxies are best fitted by a B+D model, which supports the idea described above that a cold disc structure is present.

5.1.3. Spiral arm-like residuals

KIG 599 and KIG 732 show shells and very wide spiral arm-like residuals on a very large scale. Arm-like structures are generated by an encounter that ends in a merger. The arm-like structure during the first phase, when the two nuclei are still visible, of both an encounter and a merging episode was shown in Combes et al. (1995), for instance. Clearly, KIG 732 is in an advanced merging phase. Residuals like this have been shown as residuals in other deep photometry (see e.g. Cattapan et al. 2019, in the case of NGC 1533). They were discussed as a signature of the disc instability during a merging episode (see e.g. Rampazzo et al. 2018; Mazzei et al. 2019).

5.1.4. Rings

When possible artefacts are excluded (see Sect. 4.2), several types of inner features become visible that are revealed in the residuals after model subtraction. Rings are one of the most frequent of these features, while bars are barely detected in the present sample.

Rings (inner and outer) are considered in the Buta et al. (2019) classification of isolated galaxies. Table 1 reports inner rings for four galaxies, KIG 481, KIG 490, KIG 620, and KIG 841, and a outer ring for KIG 733. The ring in KIG 481 (NGC 3682) is included in the Còmeron et al. (2014) catalogue among resonance rings in the `Spitzer` Survey of the Stellar Structure in Galaxies (S^4G), where the galaxy is classified as SA(r)0^+). After our model subtraction, the galaxy shows a strong central dust lane that perturbs the fit. It also shows concentric shell structures.

We detect inner ring-like structure in the KIG 412, KIG 517, KIG 578, KIG 620, KIG 636, KIG 637, KIG 644, KIG 685, and KIG 733 galaxies, of which seven fulfill the strict isolation spectroscopic criterion by Argudo-Fernàndez et al. (2013). In the cases of KIG 620, KIG 733, and KIG 733, which do not show obvious signatures of either interaction or merging, the rings may have been caused by resonances (Buta et al. 2010; Laurikainen et al. 2011, 2010). However, most of the detected rings are associated with other residual structures, such as shells or fan, that the literature assumes are merging signatures. Eliche-Moral et al. (2018) and Mazzei et al. (2019, and references therein) showed that the existence of embedded inner components, such as inner discs, rings, pseudo-rings, inner spirals, and nuclear bars at the centres of many S0s, which commonly are attributed to internal secular evolution, disc fading, or environmental processes, are compatible with a major-merger origin, including the relaxed and ordered discs of present-day S0s. Most of our iETGs show all these features, in combination with specific signatures of accretions/merging, such as shells. This corroborates this view.

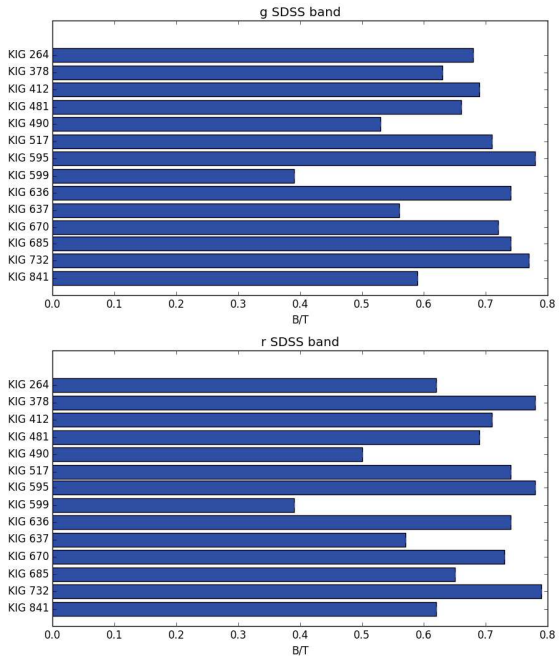

Fig. 9. Distribution of B/T in the g (*top panel*) and r bands. The average B/T values is 0.66 in both bands.

5.2. H I content

The H I content of iETGs is important for at least two reasons. On the one hand, this content is connected to the ETGs environment, and on the other, to their evolutionary scenario. More specifically, because we found so many fine structures, the H I content is essential to distinguish between the wet versus dry version of the merging episode that iETGs appear to come from.

It has been known since the early 1980s that cluster spirals are gas anæmic with respect to their counterparts in a less dense environment (see the pioneering work of Giovanelli et al. 1982). ETGs, which as a family contain less H I than spirals, have only recently been found to share this property with spirals. This has been possible through high-sensitivity surveys. A significant fraction of ETGs in a low-density environment are more H I rich than cluster ETGs (10% in Virgo vs. 40% in the field) (see e.g. Serra et al. 2012). ETGs in a low-density environment may contain as much H I as a spiral galaxy.

Serra et al. (2012) found that as far as H I properties are concerned, the main difference between ETGs with large amounts of H I and spirals is that the former miss the high column density H I that is typical of the bright stellar disc of the latter. The star formation rate per unit area is much higher in spirals than in ETGs. Instead, Serra et al. (2012) concluded that the column density of H I found in ETGs is similar to the densities observed in the outer regions of spirals, which from a morphological and kinematic point of view show warps and other peculiarities that are connected to gas accretion. Serra et al. (2012) asserted that this is what is detected in H I-rich ETGs, that is, H I-rich ETGs and spirals may look very similar in their outskirts

We investigated if those of our iETGs that show many morphological disturbances are gas rich. The sample of observed iETGs is very small. Jones et al. (2018) recently presented the largest catalogue of H I single-dish observations of isolated galaxies as part of the multi-wavelength study of the AMIGA